24th International HISWA Symposium on Yacht Design and Yacht Construction
14 and 15 November 2016, Amsterdam, The Netherlands, Amsterdam RAI Convention Centre

HYDRODYNAMICS OF WIND-ASSISTED SHIP PROPULSION
MODELLING OF HYDRODYNAMIC SIDEFORCE

N.J. van der Kolk[1], TU Delft, The Netherlands

SUMMARY

This paper deals with the hydrodynamic sideforce production of a wind-assisted ship. The subject is introduced in physical terms, and the importance of the hydrodynamic sideforce is established, before classical models are reviewed. Finally, the complications arising from diverse appendage topologies are discussed, and a theory for zero-aspect ratio lifting surfaces is discussed. The paper concludes with a short summary of ongoing work.

1. INTRODUCTION

Wind energy as an auxiliary form of propulsion for commercial ships has again become of great interest as a possible response to volatile fuel prices and increasingly stringent environmental regulations. A well-founded performance prediction tool is a key prerequisite for the further development of this promising technology, and with the support of the European Commission and others, a group of researchers at Delft University of Technology is developing a performance prediction program for these hybrid ships. The Wind-Assisted Ship Propulsion (WASP) performance prediction tool will provide designers the ability to explore the possibilities offered by wind as an auxiliary propulsor. The aim is to deliver a force model that is applicable to as broad a class of vessels as possible. This WASP modelling tool will allow for parametric investigations, and eventually for the optimisation of commercial hull forms for sailing. The expansion and refinement of the force models is the subject of ongoing work at Delft University of Technology.

This paper is organised in two parts, beginning with an introduction to the physical system and the peculiarities of wind assisted ship propulsion. This paper will then review classical models available for the hydrodynamic sideforce produced by commercial hull types and check their applicability for wind-assisted commercial vessels. The distinction between circulatory lift and sideforce generation by cross-flow drag is discussed, paying special attention to the shortcomings of these models within the present context. Interpreting the hull as a low-aspect wing-profile, an introduction to zero-aspect ratio wing theory is provided. Finally, a few topics of ongoing research that are related to sideforce modelling are presented.

1.1 Sailing Preliminaries

Fitting a commercial vessel with an auxiliary wind propulsor will introduce a set of forces and moments besides the desired aerodynamic thrust. The ship will sail with a leeway angle β about the yaw axis, which is equivalent to the angle of attack for the hull. It is this angle of attack that generates the hydrodynamic sideforce in opposition to the aerodynamic sideforce.

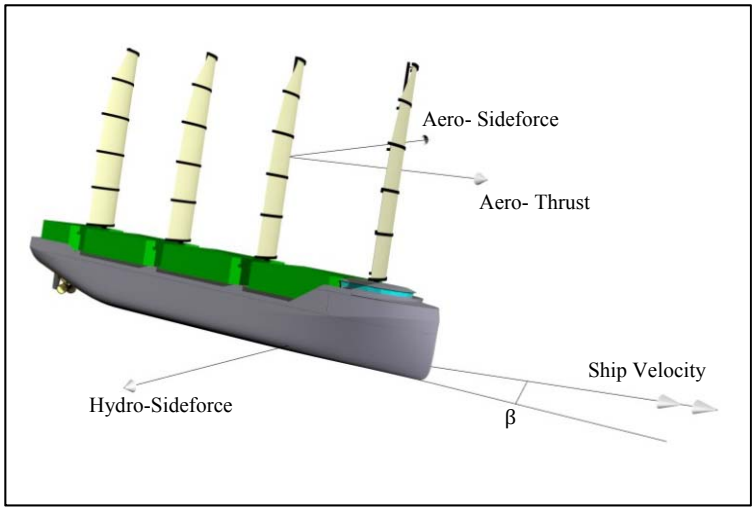

Figure 1: Schematic of wind-assist vessel, showing key force components.
Figure 2: E-Ship 1 (photo credit: **http://www.auerbach-schifffahrt.de**)

[1] n.j.vanderkolk@tudelft.nl

Further, the distribution of the hydrodynamic sideforce along the hull will result in a net yaw moment. At last, the vertical separation between the sideforce components will create a heeling moment. The steady sailing condition requires a force balance for six degrees of freedom, and a sailing ship will adopt a constant heel and leeway angle to generate the necessary reactionary forces.

In particular, the yaw balance of the ship represents a key modelling and design challenge for wind-assist vessels. A conventional commercial vessel hull—with an undersized rudder as the only appendage—is essentially unfit for sailing. Such a hull will operate with greater leeway angles, and with 'weather helm' as a consequence of this inefficient sideforce generation. The rudder can be used to oppose this destabilising moment, with an associated resistance penalty. Most of all, the vessel must still be able to manoeuvre safely. This may be a key constraint for sail plan design.

The performance of a wind-assist concept will depend on the contribution of the wind propulsor, alongside the efficiency of the conventional propulsion system. Due to the auxiliary thrust generated by the wind propulsors, the existing engine and propeller operating conditions will change. Not only will the propeller mainly operate in a light-loaded condition, but it will also operate in an oblique flow. Also to be considered is the drag penalty associated with heel and leeway: the "sailing condition". The underwater ship of a conventional freighter is ill suited for efficient sideforce production, and significant induced resistance is to be expected. Of course, the introduction of a sail-plan will only benefit the vessel if the net thrust gained outweighs any loss in efficiency or increase in resistance.

A key task is to find hull form features that can deliver the needed forces effectively and efficiently. This is a new area for commercial ships, and designers and/or owners who wish to explore the possibilities offered by wind propulsors must have a reliable and practical method for predicting performance. The influence of the sailing condition on resistance, yaw balance, propeller efficiency, stability, manoeuvrability and seakeeping all require carefully study.

1.2 Performance Prediction Program

Recognising a general lack of understanding about the physics of wind-assist vessels, and the need for an assessment tool to facilitate the further development of this promising technology, a performance prediction program is being developed at Delft University of Technology. When completed, this program will be useful throughout the design process. In early stages, when the user wants to explore several different designs, the in-built force models under development at Delft University of Technology may be used. In a more advanced design phase, the user can input data obtained by dedicated CFD calculations and experiments. In this case the program is used purely as a solver to obtain very detailed results for a specific design.

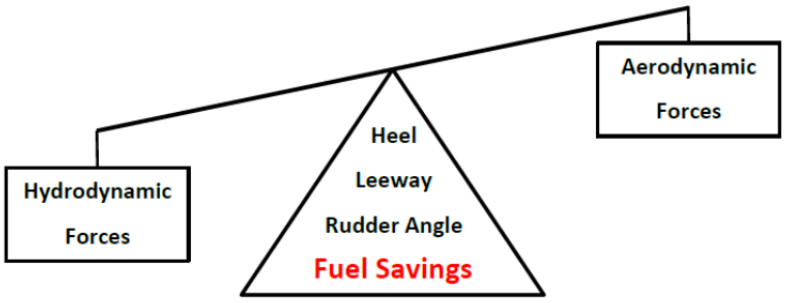

Figure 3: The force balance for the performance prediction program

The fundamental task of the PPP solver is to balance the aerodynamic and hydrodynamic forces acting on a wind-assisted ship to arrive at a sailing equilibrium. This is done within an optimization routine that maximizes the percent total thrust provided by the sail plan (thrust benefit) while maintaining a prescribed vessel speed. Alternative optimization routines may include pure sailing, delivering nominal engine power and maximizing speed, or maintaining a minimum speed. The program will calculate the performance of the wind-assisted ship for a specified range of true wind angle and true wind speed. A design can be evaluated based on these polar diagrams, or this information can be passed to a weather routing program, allowing for an environmental and economic evaluation of the wind-assisted ship under consideration. The reliable performance prediction of a wind-assisted ship is a necessary prerequisite for any sound economic and environmental evaluation of these concepts.

1.3 Uncertainty Analysis

The desired validation level for approximation methods, regression formulas, and numerical simulations must be carefully defined with the overall picture in mind. The accuracy of a performance prediction, with the interplay of several

components as outlined above is determined by the "weakest link", based on its influence on the total uncertainty. To study the sensitivity to uncertainty in hydrodynamic sideforce, take the thrust benefit (TB) as performance metric, defined as:

$$\boldsymbol{TB} \equiv 1 - \frac{X_S}{X_{tot}} \tag{1}$$

Here X_S is the aerodynamic thrust produced by the sail plan, and X_{tot} is the total resistance of the ship, including any increase due to the 'sailing condition'. This expression encapsulates the point made under 'Sailing Preliminaries': That the benefit of aerodynamics thrust must be considered against any increase in resistance or loss in efficiency. Assuming these quantities are unrelated, the associated uncertainty is:

$$U_{\boldsymbol{TB}} = \sqrt{{U_{X_{tot}}}^2 + {U_{X_S}}^2} \tag{2}$$

$U_{X_{tot}}$ is the relative error for all forces in the x-direction, and U_{X_S} is the relative error for the aerodynamic thrust. This expression does not contain the hydrodynamic sideforce.

Examining the error expression further, the aerodynamics of a wind-assisted ship is described by the ratio between aerodynamic thrust and sideforce. For the sake of argument, let us restrict our attention to a ship sailing in beam winds, so that the ratio between aerodynamic thrust and sideforce reduces to the lift to drag ratio of the rig:

$$\left(\frac{L}{D}\right)_{aero} = \frac{X_S}{Y_S} \tag{3}$$

Substituting for X_S in equation (1) gives:

$$\boldsymbol{TB} = 1 - \frac{\left(\frac{L}{D}\right)_{aero} Y_S}{X_{tot}} \tag{4}$$

Finally, recognising that the aerodynamic and hydrodynamic sideforce are equal and opposing ($Y_S = -Y_H$), the thrust benefit is now expressed in terms of the hydrodynamic sideforce:

$$\boldsymbol{TB} = 1 - \frac{\left(\frac{L}{D}\right)_{aero} (-Y_H)}{X_{tot}} \tag{5}$$

With the associated uncertainty:

$$U_{\boldsymbol{TB}} = \sqrt{{U_{X_{tot}}}^2 + \left(\frac{L}{D}\right)_{aero}^2 {U_{Y_H}}^2} \tag{6}$$

The value for $\left(\frac{L}{D}\right)_{aero}$ will vary for different rigs, apparent wind angles and speeds. Assuming a typical value of two [1], this implies that the uncertainty level for sideforce should be one quarter that for the X-equation to achieve parity among contributions to the uncertainty.

This argument can be generalised by writing equation (3) with $Y_S = -Y_H$:

$$X_S = \left(\frac{L}{D}\right)_{aero} (-Y_H) \tag{7}$$

With the associated uncertainty:

$$U_{X_S} = \left(\frac{L}{D}\right)_{aero} U_{Y_H} \tag{8}$$

It is concluded from equation (8) that the sensitivity for the sail-propulsive force to the uncertainty in hydrodynamic sideforce is equal to the aerodynamic lift-to-drag ratio. As shown in equation (7), the sideforce governs the magnitude of the aerodynamic thrust. Further, it has been shown that the uncertainty level will be a leading contributor to the overall uncertainty for the thrust benefit metric, a typical performance metric for wind-assist vessels. It is concluded, from these arguments made for beam winds, that sideforce generation is a leading force component for the assessment of a wind-assist concept.

2. MODELLING OF SIDEFORCE GENERATION

Having established the importance of the hydrodynamic sideforce with respect to the fidelity of the overall performance prediction, attention is now turned to the modelling of sideforce generation. To facilitate the ready assessment of hull performance within the context of the performance prediction tool, polynomial regression equations are derived for the sideforce from a database of systematically varied hull forms and appendage configurations. The functional form of these equations can be determined in a purely statistical way: by combining terms such that the regression residual is minimized. However, it is preferred to draw on a physical understanding of the mechanisms responsible for the generation of sideforce when forming these equations. Especially when looking beyond the boundaries of the database, where results from any regression model must be viewed critically, a function with physical underpinnings is preferred.

In the following sections, classical methods are reviewed, as applied within the study of sailing yachts and for the analysis of manoeuvring of ships. The limitations of these methods for wind-assist hull types will be discussed. Finally, a general view of sideforce production is given, concluding with a possible path forward for addressing the challenging modelling issues for sideforce generation of wind-assisted ships.

2.1 Models for Sailing Yachts

Sailing yacht hydrodynamics has been the subject of thorough study by researchers at Delft University of Technology [2] [3]. Although wind-assisted commercial ships and sailing yachts are in some ways dissimilar, there is reason to emulate the methodology of this study. These include the careful isolation of individual effects, and the application of regression analysis over an extensive database of hull geometries to create force models for an arbitrary hull form. Finally, a practical approach to the interaction between sideforce and Munk moment has been developed [4]. As outlined under 'Sailing Preliminaries', the yaw balance is expected to be a key effect for commercial ship types. A key dissimilarity between wind-assist vessels and sailing yachts is that sideforce for a sailing yacht is generated by purpose-designed appendages: the keel and rudder. The sideforce generated by these appendages is well-predicted by the lifting-line theory of Prandtl, which is reviewed below. Within the wind-assist context, such an approach is applicable to appendages with high aspect ratio, such as skegs and rudders. Finally, it is instructive as a fundamental model for the mechanisms involved in sideforce generation and the relationship between circulation and lift.

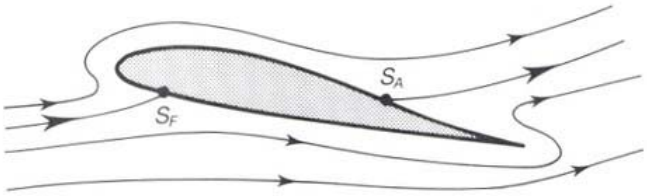

Figure 3: Wing section at $t=0^+$, immediately following an impulsive acceleration. The after stagnation point is located on the suction side. Flow passes around the trailing edge with infinite velocity.

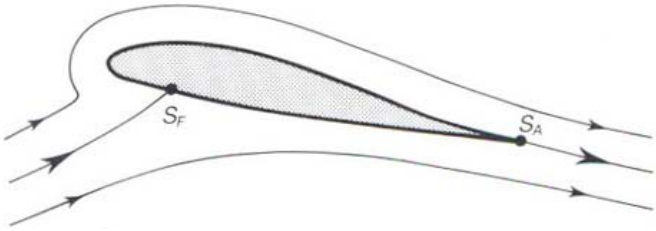

Figure 4: Wing section satisfying the Kutta condition. Vorticity production in the boundary layer is sufficient to move the after stagnation point to the trailing edge.

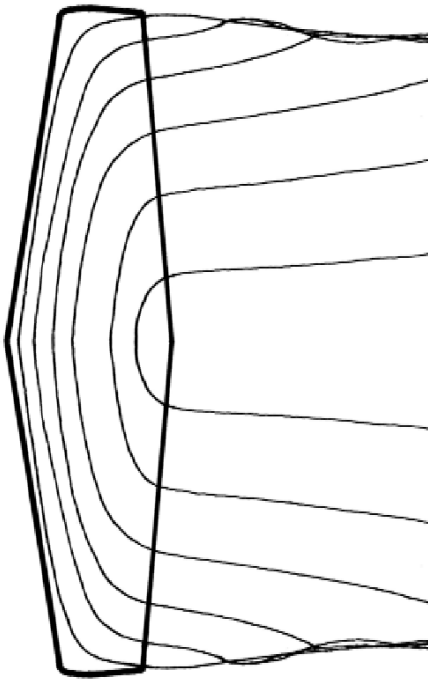

Figure 5: Wing planform showing the elaborated Prandtl vortex system. (image credits: **http://www.wikepedia.org**)

To develop Prandlt's theory, begin with a two-dimensional airfoil section oriented with an angle of attack in otherwise quiescent fluid. For the time instant immediately following an impulsive acceleration, before any boundary layer development, streamlines will pass around the sharp trailing edge with infinite flow velocity to reach the after stagnation point on the suction surface (see figure 3). As the boundary profiles fill in, the slowed flow adjacent to the foil is unable to make the turn around the trailing edge and separates, carrying vorticity produced in the boundary layer into the wake of the foil. This 'starting vortex' contributes an induced flow, acting together with a pressure gradient to bring the after stagnation point to the trailing edge of the foil (see figure 4). In the mathematical model for lifting surfaces, the singularity introduced by flow passing the sharp trailing edge is overcome with the Kutta condition. A bound circulation Γ_{Kutta} is defined to be sufficient to bring the stagnation point to the trailing edge of the foil. From the Kelvin vortex identities, the strength of this bound circulation Γ_{Kutta} is equal and opposite to the strength of the strength of the starting vortex. Finally, the sectional loading, or lift force is found by considering the change of inlet and outlet momentum due to the redirection of streamlines (see figure 4).

This analysis for the two-dimensional section was extended to the span-width by Prandtl in a famous example of asymptotic approximations. Prandtl proposed a vortex system to represent the lift generation by the foil. Prandtl's lifting line model is able to capture the viscous effects that are integral to lift generation and gives the influence of the induced flow field on the angle of attack of the foil. This is achieved by considering the inner and outer flows separately, and matching the respective asymptotic solutions. The inner solution consists of solving for the circulation necessary to satisfy the Kutta condition, as outlined above. For this approach to be valid, the aspect ratio of the foil must be sufficiently large so that span-wise derivatives can be neglected. The outer solution involves solving for the induced flow due to the trailing vortex sheet. The vorticity shed into the flow can be determined using Kelvin's identities and the span-wise variation in circulation Γ'_{Kutta}, as determined from the inner solution. This trailing vortex sheet will in turn influence the inner solution, giving a new angle of attack. Figure 5 shows a Prandtl vortex system where the bound circulation is varied in both the span- and chord-wise directions. This is a 'realistic' representation, both for the inner solution where there should be no span-wise variation, and the outer solution, where the span-wise change in circulation passes to the trailing vortices.

Before applying the results of Prandtl's analysis to wind-assist vessels, one must reconcile with the significant liberties taken when treating a hull as a foil. A key assumption underpinning the derivation outlined above is that the flow analysis can be divided into two problems according to the length scales involved. For typical ship geometries, the aspect ratio (or the draft-to-length ratio) is approximately 1/15, much smaller than the typical lower bound of applicability cited for the lifting-line theory (~3). Therefore, the scaling argument made to restrict the problem to two-dimensional planes is invalid. For ship geometries, flow characterized as 'tip effects' in Prandtl's theory, where streamlines curl around in end of the foil in response to the pressure gradient, will influence the flow pattern over the entire span (or depth of the hull). Also, a commercial hull form does not present a well-defined trailing edge, which introduces ambiguity for the definition of a circulation in the inner problem. In other words, it is not clear where (or if) the Kutta condition should be applied. These violations of the assumptions made while deriving this theory must be kept in mind when conceptualising a ship as a lifting surface and applying circulatory lift models. Still, the relationship between span-wise loading and bound circulation is useful as a basic tenant of lift generation, providing insight to the physical processes involved.

2.2 Models for Manoeuvring of Ships

The models used in the manoeuvring field are developed for ship geometries, which do not lend themselves to the assumptions made for lifting surfaces. Absent such a theoretical underpinning, forces and moments acting on the ship are written in the most general way – as hydrodynamic derivatives – to express functional dependency for combinations of body orientation and motion. For example, as utilised by Fujiwara et. al [5], the hydrodynamic sideforce for a wind-assist vessel may be written as follows:

$$Y'_H = Y'_\beta \beta + Y'_\phi \phi + Y'_{\beta\beta\beta}\beta^3 + Y'_{\beta\beta\phi}\beta^2\phi + Y'_{\beta\phi\phi}\beta\phi^2 + Y'_{\phi\phi\phi}\phi^3 \tag{9}$$

Here all forces are expressed as non-dimensional quantities according to the manoeuvring convention. It can be verified that this equation contains odd terms only, as expected for the yaw equation. The estimation of the hydrodynamic derivatives falls to a dedicated experimental test for a particular hull, or to polynomial regression formulae based on a collection of tested hulls as in [6] [7] [8] and others. Such regression equations have proven to be satisfactory for hull types that conform to the databases upon which the regressions are based.

Considering the sideforce in detail, and neglecting the influence of heel for simplicity, equation (9) may be written as the sum of linear and non-linear terms in leeway angle β:

$$Y'_H = Y'_\beta \beta + Y'_{\beta\beta\beta}\beta^3 \tag{10}$$

$$Y = Y_{lin} + Y_{non-lin} \tag{11}$$

Equation (11) is the starting point of the analysis of Hooft [9] and an attempt at synthesizing a sideforce model. His decomposition of the hydrodynamic sideforce into a linear, lifting component, and a nonlinear component due to flow separation is described below, followed by some comments regarding the utility of this approach within the wind-assist context.

Drawing a parallel with the lifting-line theory developed in Section 2.1, the first term in equation (11) is modelled as a lifting force linear in angle-of-attack β. The hull is considered to be a low-aspect-ratio wing, and the linear sideforce is written using the well-known aerodynamic model presented by Jones [10]. In particular, the lifting force is related to the rate-of-change of the fluid momentum, or virtual mass:

$$Y_{lin} = u * v \int_{AP}^{FP} \frac{dm'}{dx} dx \tag{12}$$

The virtual mass m' is otherwise known as the added mass when analyzing ship motions, where it serves to account for the momentum of fluid accelerated with the ship. Sideforce generation by a foil or by a ship, whether modelled as a circulatory lift, or as cross-flow drag, or as a combination of these effects, necessitates an equal and opposite reaction in the fluid. The generation of sideforce entails a dissipation of kinetic energy and a ship in steady sailing condition will experience a virtual mass effect, as the trailing vortices associated with sideforce production require a steady influx of energy to counter the losses due dissipation within. The sectional added mass coefficients may be readily obtained using the strip theory approach. This method, another example of matched asymptotic approximations, is briefly described here. As for the lifting-line theory, a distinction is made between longitudinal and transverse flow patterns. When the longitudinal flow scales are sufficiently larger than the transverse scales, flow confined to a transverse plane may be analyzed as a two-dimensional problem. The potential flow solution for the lateral motion, the 'inner problem', is matched with another potential satisfying the boundary conditions for the forward speed problem, the 'outer problem'. Having determined the sectional added mass from the solution to the inner problem, the integral in equation (12) is carried out over the length of the ship, and it is seen that, as an artefact of the potential flow model, the total lift will be zero. Termed the Paradox of d'Alembert, this arises because an ideal fluid will have zero added mass at the bow and stern (absent viscous wake). A three-dimensionality coefficient is introduced to resolve this matter in a practical way. It is important to pay mind to the origin of the empirical coefficient to account for viscous phenomena, as it will vary for different ship types. This concept for sectional added mass also underpins the Munk moment method of Keuning [4].

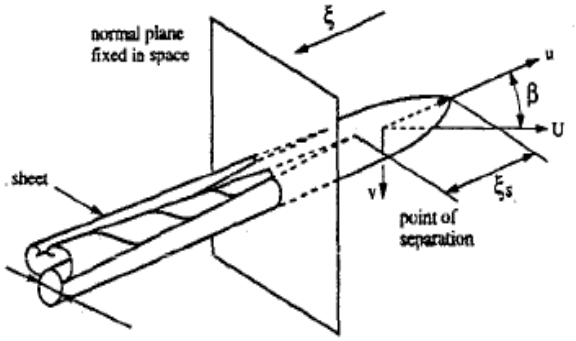

Figure 6: Sketch for analysis of flow around a cylinder at an angle of attack. The transverse plane is shown, along with the longitudinal vortices. (image credit Hooft **[11]**)

Following the analysis of Hooft [11], the non-linear term in equation (11) is the remnant after the linear component, as derived above, is subtracted from experimental results. This term is meant to represent the sideforce produced by momentum transfer as flow separates from the hull, a phenomenon known as cross-flow drag. The modelling is motivated by considering the midship section of the ship extended as an infinite beam, from which is deduced that the resulting sideforce is due to cross-flow drag only. At small leeway angles, the cross-flow drag will contribute to the sideforce according to the position of separation and the strength of the vortex sheet. In a sense, the non-linear tern is correcting for the simplifications introduced by the potential flow model and the strip theory method outlined above, where the solution for the inner problem provides values for the sectional added mass, but without the influence of upstream (or downstream) sections. Without overcomplicating the discussion, shed vortices associated with sideforce production will influence the transverse flow patterns as they pass along the ship. To segregate these effects according to a linear term that can be readily computed and a higher order remnant has a practical appeal, but somewhat obscures the physical process. The linear term

requires a three-dimensionality coefficient, accounting for viscous flow separation along the after portion of the ship, to return a non-zero sideforce for the potential solution. Further, a definition of a cross-flow drag to account for momentum transfer by longitudinal shed vortices implies a distinction between these mechanisms that is not physical. From the discussions above for circulatory lift and virtual mass, a momentum transfer is integral to any sideforce production. As a final note, the second-order sideforce component is modelled as a function of the cross-flow drag experienced by a ship with a drift angle of ninety degrees. If used as the basis for the present model, this component of sideforce is modelled in relation to a physical condition that is uncharacteristic of the flow under study.

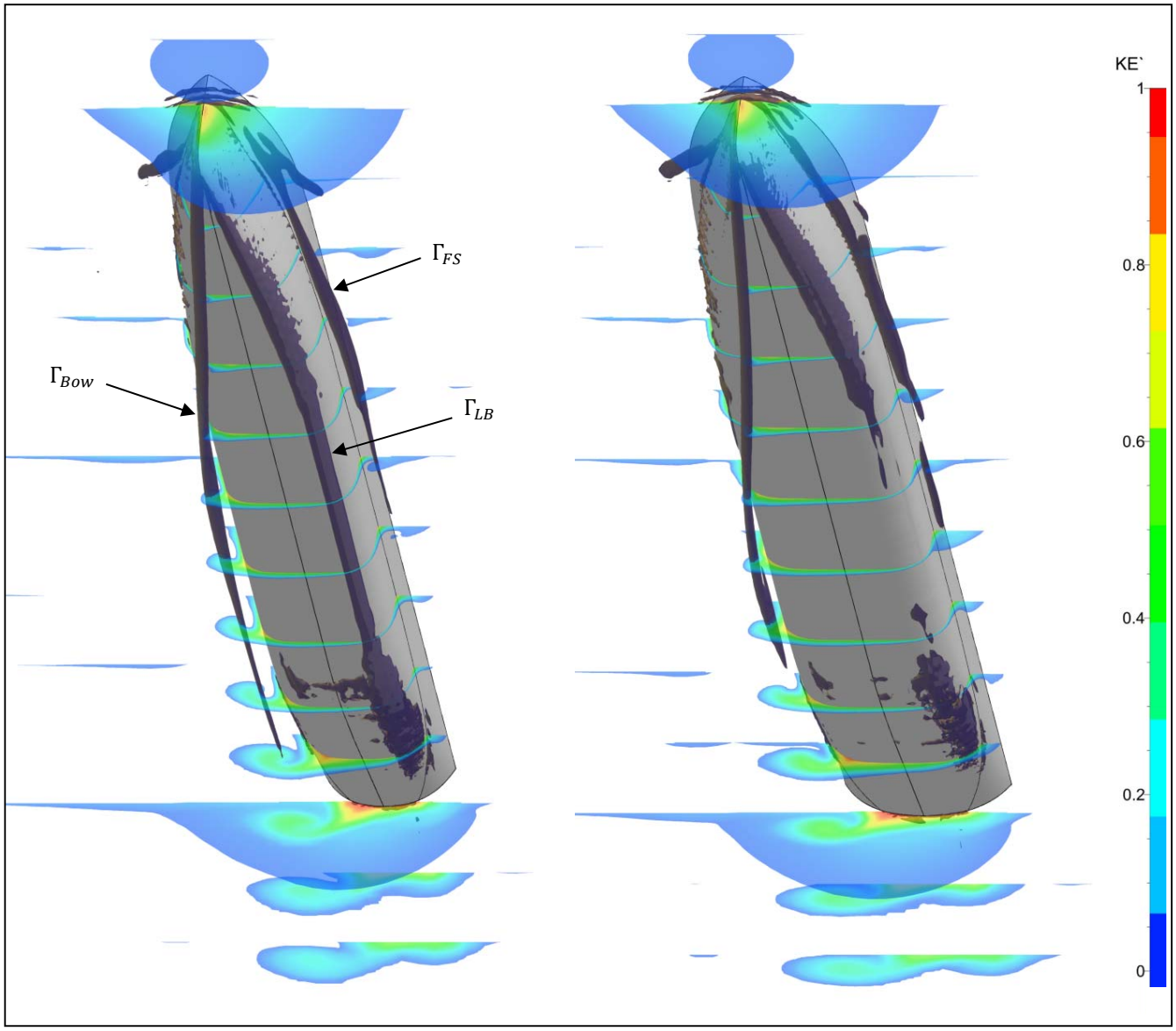

Figure 7: Numerical simulation for two wind-assist hulls with 12 knots boat speed and leeway angle equal to 9°. The orientation of the coordinate system is such that the direction of vessel motion is toward the top of the page. Longitudinal vortices are identified in dark purple, while the (normalized) fluid kinetic energy is given on transverse sections. The left hull has 20% larger T/L compared to the right hull (for the same displacement).

The vortex pattern around a hull sailing with a small leeway angle is characterized by several distinct vortices. In figure 7, they are observed passing around each hull. The hulls are oriented so the direction of vessel motion is toward the top of the page. The primary vortices are labelled with a circulation: the vortex generated at the bow Γ_{Bow}, the vortex generated at the leading bilge Γ_{LB}, and the vortex generated at the free surface Γ_{FS}. Also, a region of separation is observed at the rear

shoulder. Following the discussion in Section 2.2, the fluid kinetic energy is displayed on transverse planes. Fluid near the ship is disturbed as the ship passes. This quantity is derived from relative flow velocities and the turbulence model. It is normalized with the fluid kinetic energy at the no-slip boundary on the ship hull. Energy transferred to the fluid requires an active force, such as the ship propulsor, or the aerodynamic sideforce. Asymmetry observed in the wake of the hulls in figure 7 is evidence of the generation of a hydrodynamic sideforce in reaction to the lateral component of the aerodynamic force.

Before continuing this discussion, it must be said that while these simulations promise a detailed view of the flow behaviour around the hull, a certain uncertainty must be assigned to any quantitative analysis of these flow patterns. To that end, a rigorous validation exercise has been carried out for the integrated forces and the wave elevation along the ship. Although it is not possible to validate the flow field directly, an appreciation for the shedding patterns can motivate the structure of the regression formulas. As an example, from figure 6, one may observe that the strength of the leading bilge vortex Γ_{LB} is apparently a function of the hull aspect ratio T/L.

2.3 Generalised Sideforce Theory

For a general, appended hull, the hydrodynamic sideforce may be written as follows:

$$Y'_H = Y'_B + Y'_R + Y'_A + Y'_P \tag{13}$$

Here all forces are expressed as non-dimensional quantities in the customary manner. The sideforce has been partitioned into components arising from the **B**are hull; the **R**udder(s); components for other **A**ppendages, such as a keelson, skeg, deadwood, or bilge keels; and finally due to the primary **P**ropulsor. When speaking of sideforce generation by the bare hull, one can –when using traditional models– make a distinction between circulatory lift generation and cross-flow drag. These traditional models are illustrated as follows:

- A ship with infinite draft will generate a purely circulatory lifting force in the same way as a wing with infinite span.
- A ship with infinite length has no leading or trailing edge and thus no circulation, here the sideforce is generated by momentum transfer as vorticity is shed from the ship.

Conventional lifting surfaces, such as rudders or skegs, are well described by circulatory-lift models. The sideforce produced by the hull, or by appendages such as bilge keels, are typical examples of sideforce production by momentum transfer. Of course, the sideforce generated by a real ship will arise due to some combination of these mechanisms. For example, a high-aspect foil with finite span continually passes energy into trailing vortices. Likewise, a low-aspect rectangular planform, such as a bilge keel or a simplified hull form, develops a concentrated lifting force at the leading edge [12].

Interaction effects between the hull and appendages, and between appendages, represent a particular challenge. For example, the downwash caused by an upstream lifting surface such as a skeg will impact the angle of attack experienced by the rudder of the ship, giving a reduced lateral force. This change in angle of attack can be predicted by tracing the path of the vortices shed by the upstream wing and by working out the component of induced flow at the trailing wing. It is desirable to formulate a consistent approach that can predict the sailing performance of an appended hull for diverse appendage configurations.

An extension to zero-aspect ratio wings is described in the following. While tip-effects are incorporated with Prandtl's lifting-line theory, and so finite spans are modelled, for geometries such as bilge keels, or indeed, for the hull itself, the assumptions underlying the lifting-line theory are not respected. As the aspect ratio is reduced, it becomes necessary to model the actual distribution of vorticity along the chord length (see figure 5), and for vanishing span-width, the analysis is restricted to a single section. In an approach that began with a wing with infinite chord length, or an aspect-ratio of zero, Bollay describes an: "infinite lattice of airfoils of finite span, [...] a distribution of bound vortices of strength $\gamma(x)$ per unit length along the chord with trailing vortices leaving at some angle" [13]. For the zero-aspect-ratio wing, the bound circulation, downwash velocity, and lift are all constant across the span. Finally, as in Section 2.1, the lifting force is related to the integral of the chord-wise circulation.

Modelling the sideforce generation for a wind-assist vessel according to the vorticity distribution along length of the hull raises the possibility of elaborating the cross-flow drag models outlined above. Patterns of shedding around a hull with leeway may be characterised by a set of vortex strengths, e.g. the vortex shed at the bow, the vortex shed at the bow wave, the vortex shed at the leading bilge, and so forth. Vortices shed along the length of the hull will interact with the boundary

layer of the hull, complicating the task of modelling their path. If this is possible, the induced flow generated by the vortex system at any appendages can be predicted. Finally, the strength of these vortices may be related to (local) hull form parameters. The ability to predict the interaction effects and the ability to connect the strength of shed vorticity to (local) hull geometry are both desirable for the eventual formulation of a force model within the WASP performance prediction tool.

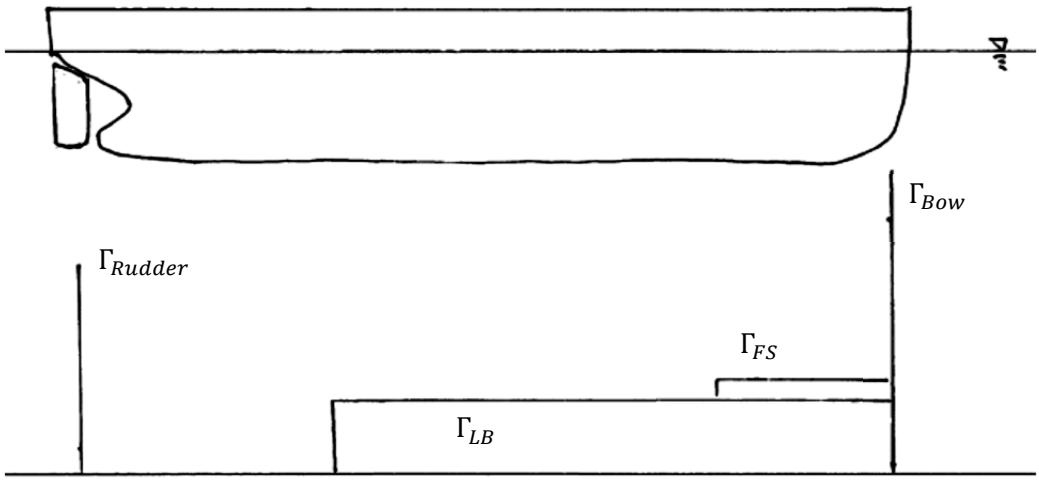

Figure 8: Example of bound vortex distribution γ(x). Components of circulation are labeled as in figure 7 above.

3. Ongoing Work

An experimental campaign was recently concluded at the TU Delft towing tank facility, the aim of which was collecting validation data for bare hull and appended cases. In addition to the Eco-liner [14] parent hull, a new hull with 10 degrees deadrise was introduced. Both hulls were tested in the bare-hull condition for a range of speeds and leeway angles. The hulls were fitted with a series of appendages: a rudder, deadwood, bilge keels, and a bar keel. They were designed to represent a broad range of appendage topologies, and to serve as validation cases for numerical tools used in the assessment of wind-assist hull hydrodynamics. The application of over-set grids for appendage investigations will allow for efficient parametric investigation of appendage arrangements. For example, the rudder can be made to move through a range of angles without requiring a new mesh or the re-computation of the entire fluid domain. In a similar fashion, the location and geometry of skegs or bilge keels can be varied. An upcoming publication will describe the experiments in detail and report the results.

Finally, as the database of hull variants is filled with validated simulation results and for diverse appendage configurations, it will be possible to test the predictive value of the models presented herein.

4. CONCLUSION

The wind-assisted commercial ship is again relevant. A sound environmental and economic evaluation of these concepts requires a reliable method for performance prediction. The hydrodynamic sideforce is a leading component of the hydrodynamics for wind-assisted ships, and presents some modelling challenges. The physical system has been described, especially the hydrodynamic sideforce that arises as a ship sails. A review of available models for the hydrodynamic sideforce was provided, along with the discussion of their merits. An approach for modelling a general appended hull was described. Finally, a brief description of ongoing work was presented.

ACKNOWLEDGEMENTS

This research is conducted with the support of the European Commission as part of the Joules Project.

BIBLIOGRAPHY

[1] G. Bordogna, J. A. Keuning, R. Huisjmans, F. V. Fossati and M. Belloli, "Validation of Simple Aerodynamic Model Capable to Predict the Interaction Effects Occurring between Two Generic Wind Propulsion Systems," in *International Conference in Hydrodynamics*, Egmond aan Zee, 2016.

[2] J. Gerritsma and R. Onnink, "Geometry, Resistance and Stability of the Delft Systematic Yacht Hull Series," *TU Delft Report # 520,* pp. 46-106, 1981.

[3] J. A. Keuning and U. B. Sonnenberg, "Approximation of the hydrodynamic forces on a sailing yacht based on the 'Delft Systematic Yacht Hull Series'," *HISWA Symposium on Yacht Design and Yacht Construction,* pp. 99-152, 1998.

[4] J. A. Keuning and K. J. Vermeulen, "The yaw balance of sailing yachts upright and heeled," *HISWA Symposium,* 2003.

[5] T. Fujiwara, G. Hearn, F. Kitamura, M. Ueno and Y. Minami, "Stead sailing performance of a hybrid-sail assisted bulk carrier," *Journal of Marine Science and Technology,* pp. 131-146, 2005.

[6] W. Jacobs, "Estimation of stability derivatives and indices of various ship forms, and comparison with experimental results," *Journal of Ship Research,* pp. 135-163, 1966.

[7] S. Inoue, H. Masayoshi and K. Katsuro, "Hydrodynamic derivatives on ship manoeuvering," *International Shipbuilding Progress,* 1981.

[8] K. Kijima, "On a prediction method of ship manoeuvring characteristics," *International Conference on Marine Simulations and Ship Manoeuverability,* 1993.

[9] J. P. Hooft, "Cross flow drag on a manoeuvring ship," *Ocean Engineering,* 1994.

[10] R. T. Jones, "Properties of low-aspect ratio pointed wings at speeds below and above the speed of sound," *NACA report # 835,* 1946.

[11] J. P. Hooft, F. Quadvlieg and . , "Non-linear hydrodynamic hull forces derived from segmented model tests," *Marine simulation and ship manoeuvrability,* pp. 399-409, 1996.

[12] J. N. Newman, Marine Hydrodynamics, Boston: MIT Press, 1977.

[13] W. Bollay, *A New Theory for Wings of Small Aspect Ratio,* Pasadena: California Institute of Technology, 1936.

[14] Dykstra Naval Architects, *Ecoliner,* Amsterdam: Dykstra Naval Architects, 2010.

[15] van Tuijl, "Evaluation of auxiliary wind propulsion system for merchant ship- Ch. ship loads," *ADEPT Report,* pp. 23-41, 2012.

[16] M. Traut, P. Gilbert, C. Bows, A. Filipone, P. Stansby and R. Wood, "Propulsive power contribution of a kite and a flettner rotor on selected shipping routes," *Applied Energy,* pp. 362-372, 2014.

[17] Y. Minami, T. Nimura, T. Fujiwara and M. Ueno, "Investigation into underwater fin arrangement effect on steady sailing characteristics of a sail assisted ship," *International Offshore and Polar Engineering Conference - Proceedings,* pp. 318-325, 2003.

[18] I. Abbot and A. Von Doenhoff, *Theory of Wind Sections,* New York: Dover Publications, 1958.

[19] MariTIM, *Wind Hybrid Coaster,* Leer, 2015.